Dynamic analysis of a fractional-order nonlinear 2-DOF vehicle system by incremental harmonic balance method

Yujian Chang
Shijiazhuang Tiedao University

Yonghao Li (405366542@qq.com)
Shijiazhuang Tiedao University https://orcid.org/0000-0002-2708-1707

Enli Chen
Shijiazhuang Tiedao University

Research Article

Keywords: Fractional-order, Nonlinear, Vehicle, IHBM

Posted Date: May 17th, 2022

DOI: https://doi.org/10.21203/rs.3.rs-1531577/v1

Dynamic analysis of a fractional-order nonlinear 2-DOF vehicle system by incremental harmonic balance method

Yujian Chang[1,a)], Yonghao Li[1,b)], Enli Chen[2]

1.School of Electrical and Electronic Engineering, Shijiazhuang Tiedao University, Shijiazhuang 050043, China

2.State Key Laboratory of Mechanical Behavior and System Safety of Traffic Engineering Structures, Shijiazhuang 050043, China

[a]Electronic mail: changyj@stdu.edu.cn\

[b]Author to whom correspondence should be addressed: 405366542@qq.com

Abstract

A two-degree-of-freedom (2-DOF) quarter vehicle fractional-order nonlinear model is presented to describe the suspension with viscoelastic material. A general calculation scheme for the 2-DOF incremental harmonic balance method (IHBM) for nonlinear systems with fractional order is derived. The nonlinear dynamic of the present model obtain is acquired by using this method. The accuracy of the proposed method is verified by comparing with the power series expansion method. Afterward, the effects of the various parameters on the dynamic performance are analyzed. Results show that the fractional-order parameters play very important roles in the amplitude-frequency response of the system.

Keywords

Fractional-order; Nonlinear; Vehicle; IHBM

1. Introduction

Suspension is an important part of the vehicle which affects the ride comfort, handling stability, safety and other performances of the vehicle. The accuracy of its model directly determines the dynamic response characteristics of the vehicle. Viscoelastic damping materials play an important role in damping and vibration control of automobile suspension. When modeling viscoelastic such as hydro pneumatic suspension, air suspension and magnetorheological suspension, it is necessary to solve the problem of dissipation force equation of viscoelastic damping material in dynamic system. The dissipative force is not only related to the historical velocity of viscoelastic material, but also transformed into a nonlinear eigenvalue problem in frequency domain[1]. Due to the fact that the fractional order model has exceptional memory function and can accurately describe the constitutive relationship of viscoelastic materials in the time domain and frequency domain[2], many scholars propose to establish the dynamic system model of viscoelastic suspension by using fractional calculus theory. Professor Alain Oustaloup[3] proposed for the first time that the damper in the traditional passive suspension should be replaced by the mechanical system with fractional damping, thus establishing the CRONE suspension. Based on the characteristics of multiphase medium mechanics of hydro pneumatic suspension, the fractional Bagley- Torvik equation was established in reference[4] and the feasibility of fractional order model in hydro pneumatic suspension system modeling was

verified by simulation and experiment. Based on the theory of fluid mechanics and the ideal gas equation of state and the advantages of fractional viscoelastic material model, the multi-branch hydro-pneumatic suspension system was modeled fractionally[5,6], then the research results showed that the use of the fractional-order model can effectively solve the damping inconsistency problem of multi-branch by changing the fractional order to observe the damping force of the suspension system. The feasibility and effectiveness of the hydropneumatic suspension model are further verified based on fractional order after comparing the fractional-order and integral-order simulation curves with the actual experimental curves.

It can be seen that the fractional-order model is more accurate than the integer-order model in studying the suspension dynamics behavior.

Nonlinearity is an important feature of automobile vertical vibration system. Many scholars have analyzed the dynamic characteristics of a 2-DOF 1/4 vehicle nonlinear model[7-11]. In terms of quantitative research, due to the strong nonlinearity and strong coupling of automobile suspension models, methods such as perturbation method, average method and multi-scale method that treat the system as weak nonlinearity are no longer applicable. Incremental harmonic balance method can study weak nonlinearity and strong nonlinearity at the same time, and the convergence accuracy can be flexibly controlled, so it has become an important method for nonlinear system research. Sheng and Wu[12] used IHBM to analyze the dynamic behavior of 2-DOF vehicle model, and obtained the steady-state periodic solution of nonlinear vehicle system. Zhou[13] used IHBM to study the quadratic and cubic stiffness and damping are contained in the suspension system and tire simultaneously. Zhou, S.H[14,15] use IHBM and Newmark-β method to compare the dynamic response of a nonlinear quarter car and, IHBM was used to study the piecewise leaf spring for the rear suspension of a truck.

It is still very rare to find the dynamics of 2-DOF systems in nonlinear automotive systems with fractional differential terms. Therefore, IHBM method is adopted in this paper to study the 2-DOF nonlinear vehicle suspension model with fractional order, to obtain its frequency response characteristics, and to analyze its dynamic characteristics and the influence of various parameters on the dynamic performance.

2. Model of Fractional-order nonlinear 2-DOF vehicle system

According to literature [20], metal rubber is a viscoelastic material, between ideal elastomer and ideal cohesive body, and its material mechanical properties are time-dependent. The elastic restoring force, the damping force with memory and the complex damping force are represented by the equivalent viscoelastic damping element, and the fractional-order differential term is introduced into the constitutive relation of metal rubber. A simple nonlinear dynamic model of metal rubber system is obtained and verified by experiments. Experimental results show that this model can accurately describe the mechanical properties of metal rubber with fewer parameters and is suitable for a wide frequency range. Its constitutive model is expressed in equation (1).

$$g(x(t),\dot{x}(t),t) = k_1^{'}x(t) + k_3^{'}x^3(t) + c_1^{'}\dot{x}(t) + h^{'}[D^p x(t)] \tag{1}$$

Where, $x(t)$ is the deformation of metal rubber spring, $k_1^{'}$ is the constant partial stiffness coefficient

of linear elastic restoring force, $k_3^{'}$ is the stiffness coefficient of cubic nonlinear elastic restoring force, $c_1^{'}$ is the first-order viscous damping coefficient, $h^{'}$ is the fractional viscoelastic damping coefficient, and p is the fractional derivative order.

There are many different definitions of fractional calculus. The definitions of Caputo and Riemann-Liouville fractional differential are shown in Equation (2) and Equation (3) respectively. Caputo type fractional calculus is used in this paper.

$$ {}_{t_0}^{C}D_t^{\,p}[x(t)] = \frac{1}{\Gamma(1-p)}\int_{t_0}^{t}\frac{x'(\tau)}{(t-\tau)^p}d\tau \tag{2} $$

$$ {}_{t_0}^{RL}\mathrm{D}_t^{p} f(t) = \frac{1}{\Gamma(n-p)}\frac{\mathrm{d}^n}{\mathrm{d}t^n}\int_{t_0}^{t}\frac{f(\tau)}{(t-\tau)^{1+p-n}}\mathrm{d}\tau \tag{3} $$

Where $\Gamma(x)$ is a Gamma function and $\Gamma(x+1) = x\Gamma(x)$.

Fig.(1) 1/4 physical model of automobile suspension including metal rubber

In this paper, metal rubber is used as the suspension material to study the 1/4 automobile suspension model. Figure (1) is the 1/4 automobile suspension system with the metal rubber instituted the oil, and a fractional nonlinear 2-dOF 1/4 automobile model is constructed according to the system, as shown in Figure (2).

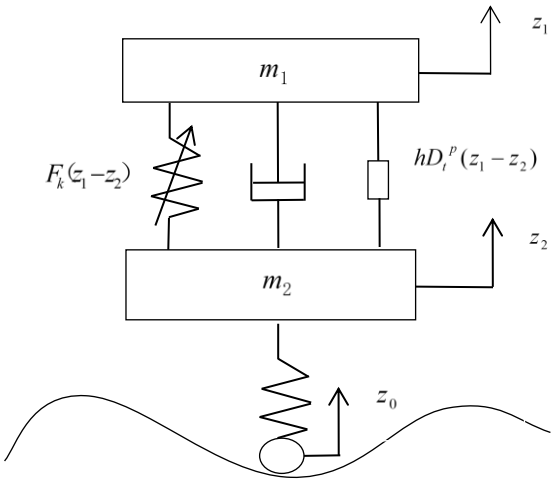

Fig.(2) Fractional order nonlinear 2-DOF suspension model

In the figure, m_1 and m_2 are the mass of the body and tire,$z_0 = F\cos(\Omega t')$ is the road excitation input, and Ω is the excitation frequency.z_1 and z_2 are tire displacement and body displacement respectively. Suspension system material is viscoelastic material, so the system includes not only nonlinear elastic restoring force and linear damping restoring force, but also viscous restoring force which is expressed by fractional order terms as follows: $\mathrm{hD_t^p(z_1 - z_2)}$, h is the coefficient of fractional differential term,$D_t^p(z_1 - z_2)$ is the $\mathrm{p}(0 \le \mathrm{p} \le 1)$derivative of $(z_1 - z_2)$ with respect to t. Capto fractional order definition is adopted in this paper.

Ignoring the higher order nonlinear elastic restoring force and higher order nonlinear damping term, the expression of nonlinear elastic restoring force is $F_k(z_1 - z_2) = k_1(z_1 - z_2) + k_3(z_1 - z_2)^3$.$k_1$ and k_3 are respectively the nonlinear spring force coefficients of suspension. The linear damping force is $c(\dot{z}_1 - \dot{z}_2)$ and c is the damping coefficient of suspension.

According to Newton's second law and the constitutive model of metal rubber, the motion differential equation of suspension system can be obtained, as shown in equation (4):

$$\begin{cases} m_1\ddot{z}_1 + k_1(z_1 - z_2) + k_3(z_1 - z_2)^3 + c(\dot{z}_1 - \dot{z}_2) + hD_t^p(z_1 - z_2) = 0 \\ m_2\ddot{z}_2 + k_t(z_2 - z_0) - k_1(z_1 - z_2) - k_3(z_1 - z_2)^3 - c(\dot{z}_1 - \dot{z}_2) - hD_t^p(z_1 - z_2) = 0 \end{cases} \tag{4}$$

Let $x_1 = z_1$, $y_1 = z_1 - z_2$.Then Formula (3) can be written as formula (5).

$$\begin{cases} m_1\ddot{x}_1 + k_1y_1 + k_3y_1^3 + c\dot{y}_1 + hD_t^py_1 = 0 \\ m_2(\ddot{x}_1 - \ddot{y}_1) + k_tx_1 - k_ty_1 - k_1y_1 - k_3y_1^3 - c\dot{y}_1 - hD_t^py_1 = k_tF\cos(\Omega t') \end{cases} \tag{5}$$

Normalize Equation (5), and let

$x = \frac{x_1}{k_tF}, y = \frac{y_1}{k_tF}, \omega_1 = \sqrt{\frac{k_1}{m_1}}, \nu = \frac{\mathrm{h}}{\mathrm{m_1}}, \omega_2 = \sqrt{\frac{k_t}{m_2}}, \mu = \frac{\mathrm{m_1}}{\mathrm{m_2}}, \delta = \frac{1}{m_2}, \gamma = \frac{k_3(k_tF)^2}{m_1}, \xi = \frac{c}{2m_1\omega_2},$

$\omega = \frac{\Omega}{\omega_1}, t = \omega_1 t'$

Then deduced (6)

$$\begin{cases} \ddot{x} + \omega_1^2y + \gamma y^3 + 2\xi\omega_2\dot{y} + \nu D_t^py = 0 \\ \ddot{x} - \ddot{y} + \omega_2^2x - \omega_2^2y - \omega_1^2\mu y - \gamma\mu y^3 - 2\xi\omega_2\mu\dot{y} - \nu\mu D_t^py = \delta\cos(\omega_t) \end{cases} \tag{6}$$

In the form of matrix: $\bar{M}\ddot{\mathrm{X}} + \bar{\mathrm{C}}\dot{\mathrm{X}} + (\bar{\mathrm{K}}_1 + \bar{\mathrm{K}}_3)\mathrm{X} + \bar{\mathrm{H}}\mathrm{D_t^pX} = \bar{\mathrm{P}}$ (7)

Where:

$\mathrm{X} = [x \quad y]^T; \bar{\mathrm{M}} = \begin{bmatrix} 1 & 0 \\ 1 & -1 \end{bmatrix}; \bar{\mathrm{C}} = \begin{bmatrix} 0 & 2\xi\omega_2 \\ 0 & -2\xi\omega_2\mu \end{bmatrix}; \bar{\mathrm{K}}_1 = \begin{bmatrix} 0 & \omega_1^2 \\ \omega_2^2 & -\omega_2^2 - \omega_1^2\mu \end{bmatrix}; \bar{\mathrm{K}}_3 = \begin{bmatrix} 0 & \gamma y^2 \\ 0 & -\gamma\mu y^2 \end{bmatrix};$

$\bar{\mathrm{H}} = \begin{bmatrix} 0 & \nu \\ 0 & -\nu\mu \end{bmatrix}; \bar{\mathrm{P}} = \begin{bmatrix} 0 \\ \delta\cos(\omega t) \end{bmatrix}$

Let:

$$\tau = \omega t,\ \mathrm{X}' = \frac{dX}{d\tau},\ \mathrm{X}'' = \frac{d^2\mathrm{X}}{d\tau^2}$$

Available:

$$\begin{cases} \dot{X} = \frac{d\mathrm{X}}{dt} = \frac{d\mathrm{X}}{d\tau}\frac{d\tau}{dt} = \omega\mathrm{X}' \\ \ddot{\mathrm{X}} = \frac{d^2\mathrm{X}}{dt^2} = \frac{d^2\mathrm{X}}{d\tau^2}\frac{d^2\tau}{dt^2} = \omega^2\mathrm{X}'' \\ D_t^p\mathrm{X} = \omega^p D_\tau^p\mathrm{X} \end{cases} \tag{8}$$

Formula (9) can be obtained by substituting formula (8) into formula (7).

$$\omega^2\bar{\mathrm{M}}\mathrm{X}'' + \omega\bar{\mathrm{C}}\mathrm{X}' + (\bar{\mathrm{K}}_1 + \bar{\mathrm{K}}_3)\mathrm{X} + \omega^p\bar{\mathrm{H}}D_\tau^p\mathrm{X} = \bar{\mathrm{P}} \tag{9}$$

3. IHBM computation scheme for fractional-order nonlinear 2-DOF

3.1 Incremental process

Suppose X_0 is the solution of the system (9) at a certain moment under the road surface excitation of fixed frequency ω, and its neighboring state can be expressed as an increment:

$$\mathrm{X} = \mathrm{X}_0 + \Delta\mathrm{X} \tag{10}$$

Where $\mathrm{X}_0 = [\mathrm{x}_0 \quad \mathrm{y}_0]^\mathrm{T},\ \Delta\mathrm{X} = [\Delta\mathrm{x} \quad \Delta\mathrm{y}]^\mathrm{T}$.

.

Formula (11) can be obtained by substituting formula (10) into formula (9) through Taylor expanding and omitting the higher order small quantities.

$$\begin{aligned} &\omega^2\bar{\mathrm{M}}\Delta\mathrm{X}'' + \omega\bar{\mathrm{C}}\Delta\mathrm{X}' + \left(\bar{\mathrm{K}}_1 + 3\bar{\mathrm{K}}_3^{(1)}\right)\Delta\mathrm{X} + \omega^p\bar{\mathrm{H}}D_\tau^p[\Delta\mathrm{X}] \\ &= \bar{\mathrm{P}} - \left\{\omega^2\bar{\mathrm{M}}\mathrm{X}''_0 + \omega\bar{\mathrm{C}}\mathrm{X}'_0 + (\bar{\mathrm{K}}_1 + \bar{\mathrm{K}}_3^{(1)})\mathrm{X}_0 + \omega^p\bar{\mathrm{H}}D_\tau^p[\mathrm{X}_0]\right\} \end{aligned} \tag{11}$$

Where $\bar{K}_3^{(1)} = \begin{bmatrix} 0 & y_0^2 \\ 0 & -k_3y_0^2 \end{bmatrix}$.

3.2 Harmonic balance process

The exact solution X_0 and the increment ΔX.Fourier expansion are shown in (12).

$$\begin{cases} x_{j0} = a_{j0} + \sum_{k=1}^{N}\left(a_{jk}\cos k\tau + b_{jk}\sin k\tau\right) \\ \Delta x_j = \Delta a_{j0} + \sum_{k=1}^{N}\left(\Delta a_{jk}\cos k\tau + \Delta b_{jk}\sin k\tau\right) \\ j = 1,2 \qquad\qquad k = 1,\ldots,N \end{cases} \tag{12}$$

Definition:

$$\mathrm{A_j} = [a_{j0},\ \ a_{j1},\ \ a_{j2},\cdots\ \ a_{jN}, b_{j1},\ \ b_{j2},\ \ \ldots\ \ , b_{jN}]^T$$
$$\Delta\mathrm{A_j} = [\Delta a_{j0},\ \ \Delta a_{j1},\ \ \Delta a_{j2},\ldots,\ \ \Delta a_{jN},\Delta b_{j1},\ \ \Delta b_{j2},\ \ \ldots,\ \ \Delta b_{jN}]^T$$
$$\mathrm{C_S} = [1,\ \ \cos\tau,\ \ \cos 2\tau,\ldots,\ \ \cos N\tau, \sin\tau\ \ \sin 2\tau,\ \ \ldots,\ \ \sin N\tau]^T$$

Let

$$S = \begin{bmatrix} \mathrm{C_S} & 0 \\ 0 & \mathrm{C_S} \end{bmatrix}; A = \begin{bmatrix} \mathrm{A_1} \\ \mathrm{A_2} \end{bmatrix}; \Delta\mathrm{A} = \begin{bmatrix} \Delta\mathrm{A_1} \\ \Delta\mathrm{A_2} \end{bmatrix}$$

Then the exact solution and increment can be expressed as formula (13)

$$\begin{cases} \mathrm{X}_0 = SA \\ \Delta\mathrm{X} = S\Delta A \end{cases} \tag{13}$$

When the Galerkin average process is applied to the integration of formula (11), the fractional differential term is aperiodic function, so the fractional differential term should be integrated and averaged within the period T(T=∞), and the period of other functions is 2π. Therefore, by integrating in 2π, equation (14) can be obtained.

$$\begin{aligned} &\tfrac{1}{2\pi}\int_0^{2\pi}(\delta\Delta\mathrm{X})^{\mathrm{T}}\begin{bmatrix}\omega^2\overline{\mathrm{M}}\Delta\mathrm{X}'' + \omega\overline{\mathrm{C}}\Delta\mathrm{X}' \\ +(\overline{\mathrm{K}}_1 + 3\overline{\mathrm{K}}_3^{(1)})\Delta X\end{bmatrix}d\tau + \tfrac{1}{T}\int_0^T(\delta\Delta\mathrm{X})^{\mathrm{T}}\{\,\omega^p\overline{\mathrm{H}}D_\tau^p[\Delta\mathrm{X}]\}d\tau \\ &= \tfrac{1}{2\pi}\int_0^{2\pi}(\delta\Delta\mathrm{X})^{\mathrm{T}}\left\{\overline{\mathrm{P}} - \begin{bmatrix}\omega^2\overline{\mathrm{M}}\mathrm{X}''_0 + \omega\overline{\mathrm{C}}\mathrm{X}'_0 \\ +(\overline{\mathrm{K}}_1 + \overline{\mathrm{K}}_3^{(1)})\mathrm{X}_0\end{bmatrix}\right\}d\tau - \tfrac{1}{T}\int_0^T(\delta\Delta\mathrm{X})^{\mathrm{T}}\{\,\omega^p\overline{\mathrm{H}}D_\tau^p[\mathrm{X}_0]\}d\tau \end{aligned} \tag{14}$$

By substituting equation (13) into integral equation (14) to get equation (15).

$$\begin{aligned} &(\delta\Delta\mathrm{A})^{\mathrm{T}}\left\{\tfrac{1}{2\pi}\int_0^{2\pi}\mathrm{S}^{\mathrm{T}}\left[\omega^2\overline{\mathrm{M}}\mathrm{S}'' + \omega\overline{\mathrm{C}}\mathrm{S}' + (\overline{\mathrm{K}}_1 + 3\overline{\mathrm{K}}_3^{(1)})\mathrm{S}\right]d\tau\right\}\Delta\mathrm{A} + (\delta\Delta\mathrm{A})^{\mathrm{T}}\left\{\tfrac{1}{T}\int_0^T(\mathrm{S})^{\mathrm{T}}\,\omega^p\overline{\mathrm{H}}D_\tau^p[\mathrm{S}]d\tau\right\}\Delta\mathrm{A} \\ &= (\delta\Delta\mathrm{A})^{\mathrm{T}}\tfrac{1}{2\pi}\int_0^{2\pi}\mathrm{S}^{\mathrm{T}}\left\{\overline{\mathrm{P}} - \left[\omega^2\overline{\mathrm{M}}\mathrm{S}'' + \omega\overline{\mathrm{C}}\mathrm{S}' + (\overline{\mathrm{K}}_1 + \overline{\mathrm{K}}_3^{(1)})\mathrm{S}\right]\mathrm{A}\right\}d\tau - (\delta\Delta\mathrm{A})^{\mathrm{T}}\left\{\tfrac{1}{T}\int_0^T(\mathrm{S})^{\mathrm{T}}\{\,\omega^p\overline{\mathrm{H}}D_\tau^p[\mathrm{S}]d\tau\}\mathrm{A}\right\} \end{aligned} \tag{15}$$

Furthermore the formula(16)is obtained:

$$\begin{aligned} &\left\{\tfrac{1}{2\pi}\int_0^{2\pi}\mathrm{S}^{\mathrm{T}}\begin{bmatrix}\omega^2\overline{\mathrm{M}}\mathrm{S}'' + \omega\overline{\mathrm{C}}\mathrm{S}' \\ +(\overline{\mathrm{K}}_1 + 3\overline{\mathrm{K}}_3^{(1)})\mathrm{S}\end{bmatrix}d\tau + \tfrac{1}{T}\int_0^T\mathrm{S}^{\mathrm{T}}\,\omega^p\overline{\mathrm{H}}D_\tau^p[\mathrm{S}]d\tau\right\}\Delta A \\ &= \tfrac{1}{2\pi}\int_0^{2\pi}\mathrm{S}^{\mathrm{T}}\left[\overline{\mathrm{P}} - \begin{bmatrix}\omega^2\overline{\mathrm{M}}\mathrm{S}'' + \omega\overline{\mathrm{C}}\mathrm{S}' \\ +(\overline{\mathrm{K}}_1 + \overline{\mathrm{K}}_3^{(1)})\mathrm{S}\end{bmatrix}\mathrm{A}\right]d\tau - \left\{\tfrac{1}{T}\int_0^T\mathrm{S}^{\mathrm{T}}\{\,\omega^p\overline{\mathrm{H}}D_\tau^p[\mathrm{S}]\}\mathrm{A}d\tau\right\} \end{aligned}$$

(16)

Get a linear group of equations of ΔA

$$\mathrm{N}\Delta\mathrm{A} = \mathrm{R} \tag{17}$$

Where:

$$N = \mathrm{N}_1 + \mathrm{N}_2^p$$

$$\mathrm{N}_1 = \frac{1}{2\pi}\left\{\omega^2 \int_0^{2\pi} \mathrm{S}^{\mathrm{T}}\bar{\mathrm{M}}\mathrm{S}''d\tau + \omega\int_0^{2\pi} \mathrm{S}^{\mathrm{T}}\bar{\mathrm{C}}\mathrm{S}'d\tau + \int_0^{2\pi} \mathrm{S}^{\mathrm{T}}(\bar{\mathrm{K}}_1 + 3\bar{\mathrm{K}}_3^{(1)})\mathrm{S}d\tau\right\}$$

$$\mathrm{N}_2^p = \frac{\omega^p 1}{T}\int_0^T \mathrm{S}^{\mathrm{T}}\,\bar{\mathrm{H}}D_\tau^p[\mathrm{S}]d\tau$$

$$R = \mathrm{R}_1 + \mathrm{R}_2^p$$

$$R_1 = \frac{1}{2\pi}\left\{\int_0^{2\pi} \mathrm{S}^{\mathrm{T}}\bar{\mathrm{P}}d\tau - \left[\omega^2 \int_0^{2\pi} \mathrm{S}^{\mathrm{T}}\bar{\mathrm{M}}\mathrm{S}''d\tau + \omega\int_0^{2\pi} \mathrm{S}^{\mathrm{T}}\bar{\mathrm{C}}\mathrm{S}'d\tau + \int_0^{2\pi} \mathrm{S}^{\mathrm{T}}(\bar{\mathrm{K}}_1 + \bar{\mathrm{K}}_3^{(1)})\mathrm{S}d\tau\right] \times A\right\}$$

$$R_2^p = -\frac{\omega^p}{T}\int_0^T \mathrm{S}^{\mathrm{T}}\,\bar{\mathrm{H}}D_\tau^p[S]d\tau \times A$$

N_1 and R_1 are iteration formats of integer order differential terms in IHBM, which can be calculated by directly substituting parameters into the calculation, while N_2^p and R_2^p contain fractional order differential terms and their corresponding parts in IHBM.

First, simplify N_2^p as formula (18).

$$N_2^{\mathrm{P}} = \frac{\omega^p}{T}\int_0^T \mathrm{S}^{\mathrm{T}}\,\bar{\mathrm{H}}D_\tau^p[\mathrm{S}]d\tau \tag{18}$$

$$= \frac{\omega^p}{T}\int_0^T \begin{bmatrix}\mathrm{C}_{\mathrm{S}}^{\mathrm{T}} & 0\\ 0 & \mathrm{C}_{\mathrm{S}}^{\mathrm{T}}\end{bmatrix}\begin{bmatrix}0 & \nu\\ 0 & -\nu\mu\end{bmatrix} D_\tau^p \begin{bmatrix}\mathrm{C}_{\mathrm{S}} & 0\\ 0 & \mathrm{C}_{\mathrm{S}}\end{bmatrix} d\tau$$

$$= \frac{\omega^p}{T}\int_0^T \begin{bmatrix}0 & \nu\mathrm{C}_{\mathrm{S}}^{\mathrm{T}}\\ 0 & -\nu\mu\mathrm{C}_{\mathrm{S}}^{\mathrm{T}}\end{bmatrix}\begin{bmatrix}D_\tau^p\mathrm{C}_{\mathrm{S}} & 0\\ 0 & D_\tau^p\mathrm{C}_{\mathrm{S}}\end{bmatrix} d\tau$$

$$= \frac{\omega^p}{T}\int_0^T \begin{bmatrix}0 & \nu\mathrm{C}_{\mathrm{S}}^{\mathrm{T}}D_\tau^p\mathrm{C}_{\mathrm{S}}\\ 0 & -\nu\mu\mathrm{C}_{\mathrm{S}}^{\mathrm{T}}D_\tau^p\mathrm{C}_{\mathrm{S}}\end{bmatrix} d\tau$$

$$= \begin{bmatrix}0 & \mathrm{M}_2^p\\ 0 & -\mu\mathrm{M}_2^p\end{bmatrix}$$

M_2^p can be written as (19):

$$M_2^{\mathrm{P}} = \frac{\omega^p}{T}\int_0^T \nu\mathrm{C}_{\mathrm{S}}^{\mathrm{T}}D_\tau^p C_{\mathrm{S}}\,d\tau = \begin{bmatrix}[\mathrm{M}_{11}]^P & [\mathrm{M}_{12}]^P\\ [\mathrm{M}_{21}]^P & [\mathrm{M}_{22}]^P\end{bmatrix}$$

(19)

In Formula

$$[M_{11}]_{ij}^{p} = \lim_{T\to\infty}\frac{1}{T}\int_0^T \nu\omega^p \cos i\tau D_\tau^p[\cos j\tau]d\tau \quad i = 0,1,\ldots,N \qquad j = 0,1,\ldots,N \tag{20a}$$

$$[\mathrm{M}_{12}]_{ij}^{p} = \lim_{T\to\infty}\frac{1}{T}\int_0^T \nu\omega^p \cos i\tau D_\tau^p[\sin j\tau]d\tau \quad i = 0,1,\ldots,N \qquad j = 1,\ldots,N \tag{20b}$$

$$[M_{21}]_{ij}^{p} = \lim_{T\to\infty}\frac{1}{T}\int_0^T \nu\omega^p \sin i\tau D_\tau^p[\cos j\tau]d\tau \quad i = 1,\ldots,N \qquad j = 0,1,\ldots,N \tag{20c}$$

$$[M_{22}]_{ij}^{p} = \lim_{T\to\infty}\frac{1}{T}\int_0^T \nu\omega^p \sin i\tau D_\tau^p[\sin j\tau]d\tau \quad i = 1,\ldots,N \qquad j = 1,\ldots,N \tag{20d}$$

According to the definition of Captuto type calculus, and power series expansion method formula (21) can be calculated according to reference [16].

$$[\mathrm{M}_{11}]_{ij}^{p} = \lim_{T\to\infty}\frac{1}{T}\int_0^T \nu\,\omega^p \cos i\tau D_\tau^p[\cos j\pi]d\tau = \lim_{T\to\infty}\frac{1}{T}\int_0^T \left\{\nu\omega^p \cos i\tau \times \left[\frac{1}{\Gamma(1-p)}\int_0^\tau \frac{-j\sin ju}{(\tau-u)^p}du\right]\right\}d\tau \tag{21}$$

Formula (21) becomes (22) by introducing $\mathrm{s} = \tau - \mathrm{u}$ and $\mathrm{du} = -\mathrm{ds}$.

$$[M_{11}]_{ij}^{p} = \frac{-j\nu\omega^p}{\Gamma(1-p)}\lim_{T\to\infty}\frac{1}{T}\int_0^T \left\{\cos i\tau \times \left[\int_0^\tau \frac{\sin(j\tau - js)}{s^p}ds\right]\right\}d\tau \tag{22}$$

$$= \frac{-j\nu\omega^p}{\Gamma(1-p)}\lim_{T\to\infty}\frac{1}{T}\int_0^T [\cos i\tau \sin j\tau \int_0^\tau \frac{\cos js}{s^p}ds]d\tau + \frac{-j\nu\omega^p}{\Gamma(1-p)}\lim_{T\to\infty}\frac{1}{T}\int_0^T [\cos i\tau \cos j\tau \int_0^\tau \frac{\sin js}{s^p}ds]d\tau$$

For definitions (22), the first part is A_1 and the second part is A_2. Formulas (23) and (24) can be obtained by integration by parts.

$$\mathbf{A}_1 = \frac{-j\nu\omega^p}{\Gamma(1-p)}\lim_{T\to\infty}\frac{1}{T}\int_0^T \left\{\frac{1}{2}[\sin(i+j)\tau - \sin(i-j)\tau]\int_0^\tau \frac{\cos js}{s^p}ds\right\}d\tau \tag{23}$$

$$= \frac{-j\nu\omega^p}{2\Gamma(1-p)}\lim_{T\to\infty}\frac{1}{T}\left[\frac{\cos(i+j)\tau}{(i+j)} - \frac{\cos(i-j)\tau}{(i-j)}\right]\int_0^\tau \frac{\cos js}{s^p}ds|_0^T$$

$$-\frac{j\nu\omega^p}{2\Gamma(1-p)}\lim_{T\to\infty}\frac{1}{T}\int_0^T \left[\frac{\cos(i+j)\tau}{(i+j)} - \frac{\cos(i-j)\tau}{(i-j)}\right]\frac{\cos j\tau}{\tau^p}d\tau$$

$$A_2 = \frac{j\nu\omega^p}{\Gamma(1-p)}\lim_{T\to\infty}\frac{1}{T}\int_0^T \left\{\frac{1}{2}[\cos(i+j)\tau + \cos(i-j)\tau]\int_0^\tau \frac{\sin js}{s^p}ds\right\}d\tau \tag{24}$$

$$= \frac{j\nu\omega^p}{2\Gamma(1-p)}\lim_{T\to\infty}\frac{1}{T}\int_0^T \left[\frac{\sin(i+j)\tau}{(i+j)} + \frac{\sin(i-j)\tau}{(i-j)}\right]\int_0^\tau \frac{\sin js}{s^p}ds|_0^T$$

$$-\frac{j\nu\omega^p}{2\Gamma(1-p)}\lim_{T\to\infty}\frac{1}{T}\int_0^T \left[\frac{\sin(i+j)\tau}{(i+j)} + \frac{\sin(i-j)\tau}{(i-j)}\right]\frac{\sin j\tau}{\tau^p}d\tau$$

Let the first part of A_1 be B_{A11}, the second part be B_{A12}, the first part of A_2 be B_{A21}, and the second part be B_{A22}.

According to the two basic formulas (25) in the literature [19-21]:

$$\lim_{T\to\infty}\int_0^T \frac{\sin(js)}{s^p}ds = j^{p-1}\Gamma(1-p)\cos(\frac{p\pi}{2}) \tag{25a}$$

$$\lim_{T\to\infty}\int_0^T \frac{\cos(js)}{s^p}dt = j^{p-1}\Gamma(1-p)\sin(\frac{p\pi}{2}) \tag{25b}$$

Substitute (25) formula into (23), (24) and obtain (26), (27).

$$B_{\mathrm{A11}} = \frac{\nu\omega^p j^p \sin(\frac{p\pi}{2})}{2}\lim_{T\to\infty}\frac{1}{T}\times[\frac{\cos(i+j)T}{(i+j)} - \frac{\cos(i-j)T}{(i-j)}] = 0 \tag{26a}$$

$$\mathrm{B_{A12}} = -\frac{j\nu\omega^p}{2\Gamma(1-p)}\lim_{T\to\infty}\frac{1}{T}\int_0^T\left[\frac{\cos(i+j)\tau\cos j\tau}{(i-j)\tau^p} - \frac{\cos(i-j)\tau\cos j\tau}{(i-j)\tau^p}\right]d\tau = 0 \tag{26b}$$

$$\mathrm{B_{A21}} = \frac{\nu\omega^p j^p \cos(\frac{p\pi}{2})}{2}\lim_{T\to\infty}\frac{1}{T}\times[\frac{\sin(i+j)T}{(i+j)} + \frac{\sin(i-j)T}{(i-j)}] = \begin{cases} 0, & i\neq j \\ \dfrac{\nu\omega^p j^p \sin(\frac{p\pi}{2})}{2}, & i=j \end{cases} \tag{27a}$$

$$\mathrm{B_{A22}} = -\frac{j\nu\omega^p}{2\Gamma(1-p)}\lim_{T\to\infty}\frac{1}{T}\int_0^T\left[\frac{\sin(i+j)\tau\sin j\tau}{(i+j)\tau^p} + \frac{\sin(i-j)\tau\sin j\tau}{(i-j)\tau^p}\right]d\tau = 0 \tag{27b}$$

The simultaneous equations (22) to (27) can be used to calculate M_{11}. Similarly, M_{12}, M_{21}, M_{22} and M_{22} can be obtained. As shown in formula (28).

$$[\mathrm{M_{11}}]_{ij}^p = \begin{cases} 0, & i\neq j \\ \dfrac{\nu\omega^p j^p \cos(\frac{p\pi}{2})}{2}, & i=j \end{cases} \tag{28a}$$

$$[\mathrm{M_{12}}]_{ij}^p = \begin{cases} 0, & i\neq j \\ \dfrac{\nu\omega^p j^p \sin(\frac{p\pi}{2})}{2}, & i=j \end{cases} \tag{28b}$$

$$[\mathrm{M_{21}}]_{ij}^p = \begin{cases} 0, & i\neq j \\ \dfrac{-\nu\omega^p j^p \sin(\frac{p\pi}{2})}{2}, & i=j \end{cases} \tag{28c}$$

$$[\mathrm{M_{22}}]_{ij}^p = \begin{cases} 0, & i\neq j \\ \dfrac{\nu\omega^p j^p \cos(\frac{p\pi}{2})}{2}, & i=j \end{cases} \tag{28d}$$

Expansion (28) gives the form (29):

$$[\mathrm{M}_{11}]^P = \frac{\nu\omega^p \cos(\frac{p\pi}{2})}{2}\begin{bmatrix} 0^p & 0 & \cdots & 0 \\ 0 & 1^p & \cdots & 0 \\ \vdots & \vdots & \ddots & \vdots \\ 0 & 0 & \cdots & N^P \end{bmatrix}_{(N+1)\times(N+1)} \tag{29a}$$

$$[\mathrm{M}_{12}]^P = \frac{\nu\omega^p \sin(\frac{p\pi}{2})}{2}\begin{bmatrix} 0 & 0 & \cdots & 0 \\ 1^p & 0 & \cdots & 0 \\ \vdots & \vdots & \ddots & \vdots \\ 0 & 0 & \cdots & N^P \end{bmatrix}_{(N+1)\times N} \tag{29b}$$

$$[\mathrm{M}_{21}]^P = \frac{\nu\omega^p sin(\frac{p\pi}{2})}{2}\begin{bmatrix} 0 & -1^p & \cdots & 0 \\ 0 & 0 & \cdots & 0 \\ \vdots & \vdots & \ddots & \vdots \\ 0 & 0 & 0 & -N^P \end{bmatrix}_{N\times(N+1)} \tag{29c}$$

$$[M_{22}]^P = \frac{\nu\omega^p \cos(\frac{p\pi}{2})}{2}\begin{bmatrix} 1^p & 0 & \cdots & 0 \\ 0 & 2^p & \cdots & 0 \\ \vdots & \vdots & \ddots & \vdots \\ 0 & 0 & 0 & N^P \end{bmatrix}_{N\times N} \tag{29d}$$

The iteration formula of N_2^p is obtained from the above equation, and similarly, the iteration formula of R_2^p is obtained.

Thus, according to equation (16), when the initial value A_0 is given, loop iteration is carried out until the precision requirements are met. Therefore, the periodic approximate solution of arbitrary precision of the system can be obtained. The solution process is shown in Figure (3).

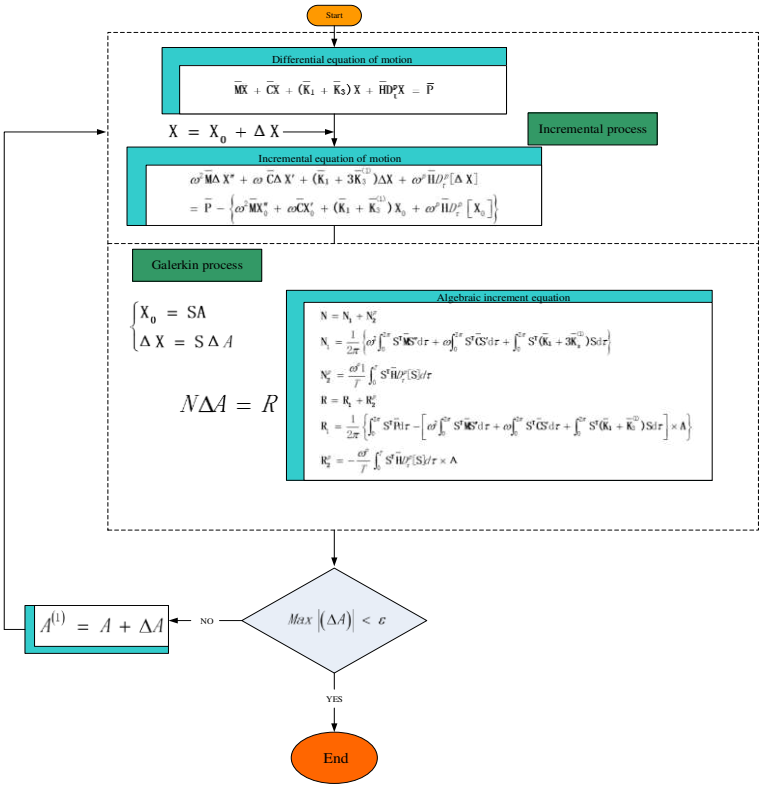

Fig.(3)Incremental harmonic balance calculation process

Table 1 Simulation parameters

suspension parameters	numerical value	suspension parameters	numerical value
m_1/kg	240	k_3/(N·m^{-1})	10000
m_2/kg	30	c/(N·s·m^{-1})	1000
k_1/(N·m^{-1})	16000	h	1000
k_t/(N·m^{-1})	160000	p	0.5

4. Simulation results and discussions

4.1 Harmonics number selection and result verification

The number of harmonics directly affects the accuracy of steady-state response. The higher the number N, the higher the accuracy of calculation, but the longer the calculation time is. So the compromise between the number of harmonics is needed. In this paper, N=4,5,6 are selected for calculation. The simulation parameters are in Table 1. Comparison of the calculated results is shown in Fig. (4). The deviation of amplitude-frequency response curve is large when N=4 and N=5, but small when N=5 and N=6. The magnitude of the deviation after enlarging the image is only 10^{-6} times, indicating that the accuracy of N=5 is very high. Therefore, this paper chooses the result of N=5 for analysis and research, which can guarantee the accuracy requirement with faster calculation speed.

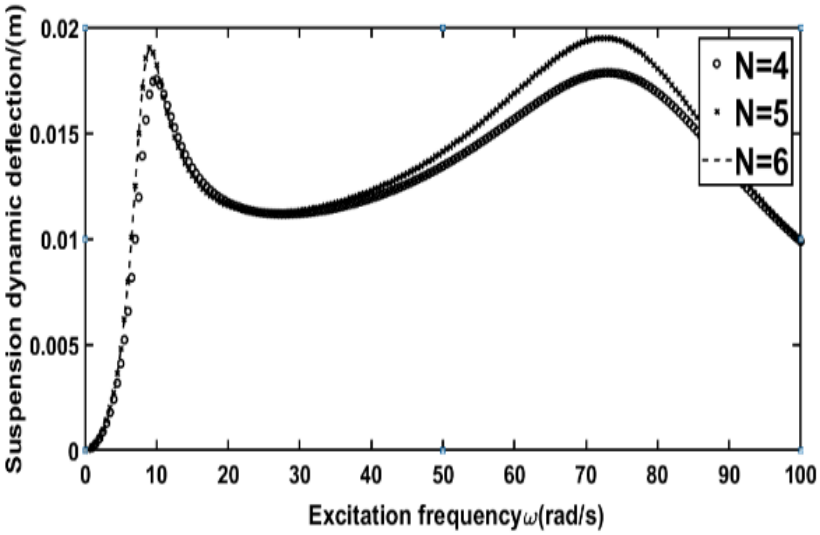

a) Body displacement amplitude-frequency response curve

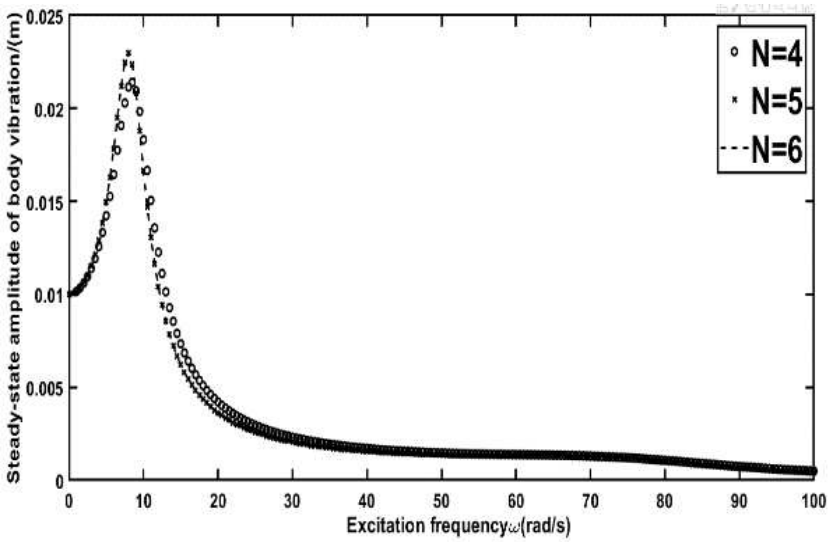

b) Amplitude-frequency response of suspension dynamic deflection

Fig.(4) Amplitude-frequency response curves with different harmonic numbers

Generally, the Runge-kutta or Newmark methods are used for integer order numerical calculation, but they are no longer applicable when the system contains fractional order. The power series expansion method is used for numerical simulation, in which the step size is $\frac{\pi}{100\omega}$, 300 cycles are calculated, and the maximum amplitude of the next 150 cycles is taken as the stable amplitude. The simulation flow chart is shown in figure (5).

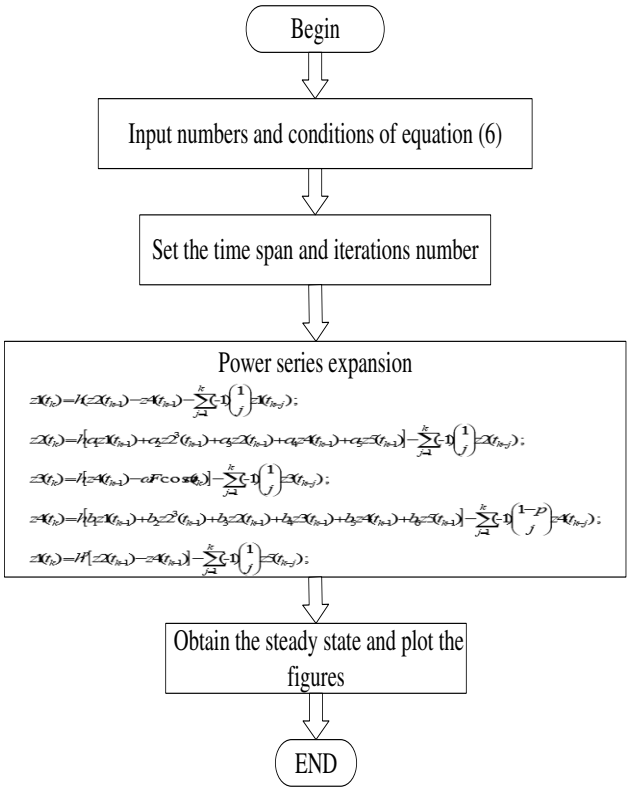

Fig.(5) Simulation flow chart of power series expansion method

The IHBM results are compared with the numerical simulation results, as shown in Figure (6). It can be seen that IHMB is in fairly adequate agreement with the results calculated through numerical method at the amplitude of spring mass vibration.

Although there is a slight difference between IHBM and numerical method in mid and high frequency of suspension dynamic deflection, but it remains within a very narrow margin. Therefore, the two-degree-of-freedom IHBM algorithm with fractional order is feasible and has high accuracy.

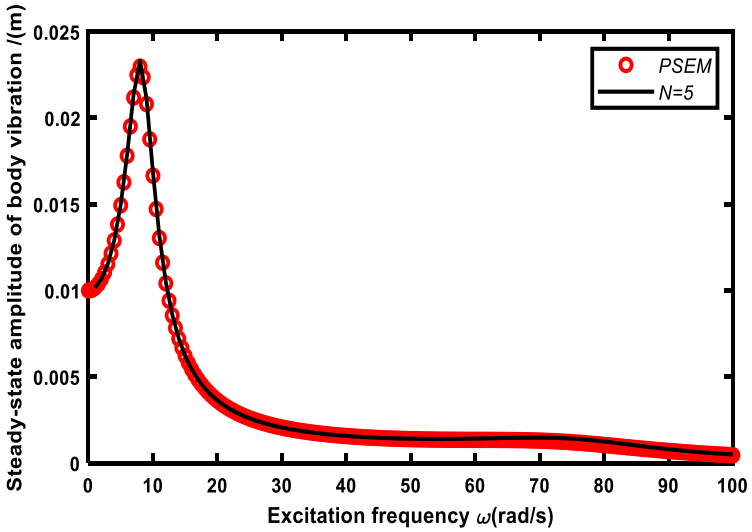

a) Amplitude-frequency response curve of body displacement

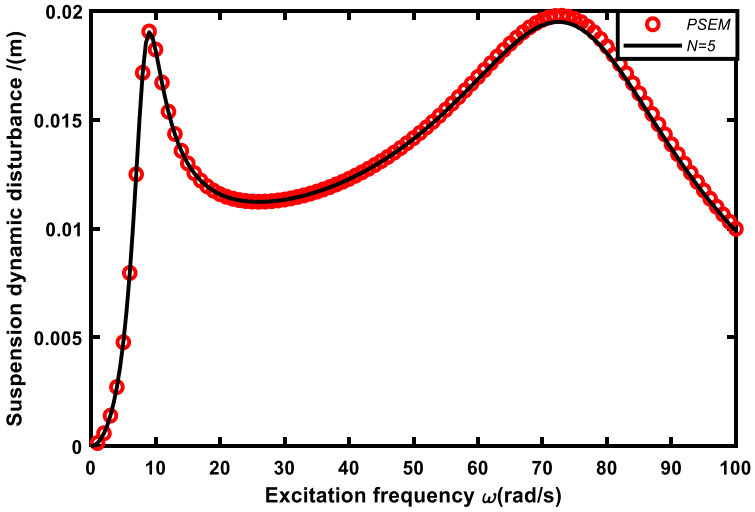

b) Amplitude-frequency response of suspension dynamic deflection

Fig.(6) Comparison of amplitude-frequency response curves of PSEM and IHBM

4.2 Influence of fractional order parameters on dynamic performance of vehicle suspension system

When the system contains fractional order differential term, there are two special parameters. One is the order of differential term and the other is coefficient of differential term. Their effects on the dynamic performance of the system is studied respectively.

(1)Effect of the fractional order on dynamic behavior of vehicle system

The system takes the fractional order of 0,0.2,0.4,0.6,0.8 and 1.0 to study. The body vibration amplitude-frequency response curve after changing the system parameters is shown in Fig. (7). As can be seen from the figure, the lower the fractional order, the higher the vibration amplitude of the system and the higher the resonance peak value, which is consistent with the physical meaning that the lower the fractional order, the greater the proportion of the stiffness part and the lower the proportion of the damping part.

There is an obvious contrast between the amplitude-frequency response curves of the fractional order and the ones of the interger order, a fact which indicates that the fractional order differential term is more accurate for describing the system and closer to the actual system.

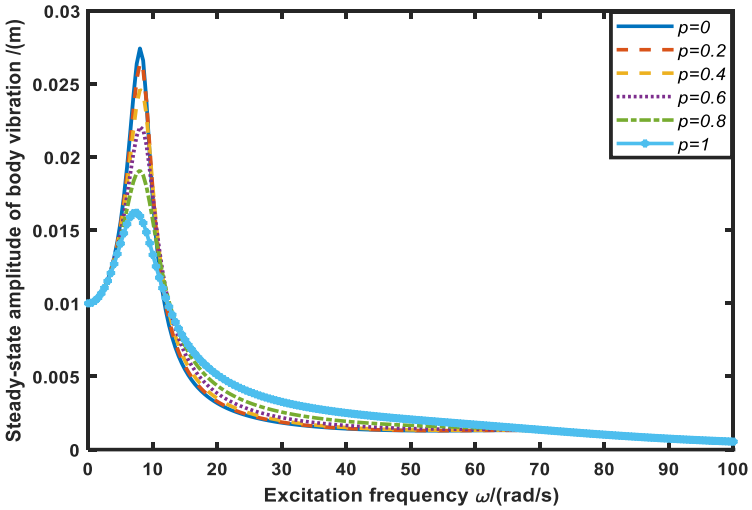

a) Amplitude-frequency response curve of body displacement

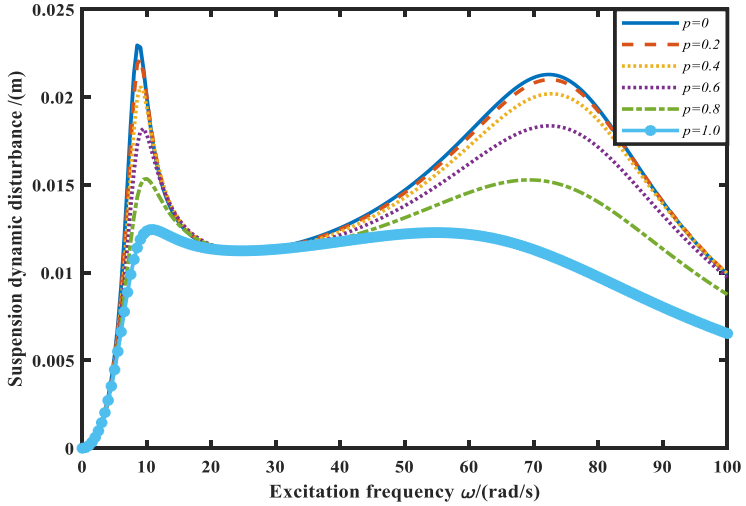

b) Amplitude-frequency response of suspension dynamic deflection

Fig.(7)Comparison of amplitude-frequency responses of different fractional orders

(2)Effect of fractional coefficient on dynamic behavior of vehicle system

The fractional differential coefficients of 500, 1000, 1500 and 2000 were respectively used in the system for research. The amplitude-frequency response curve of body vibration when the system changes parameters is shown in Figure (8). It can be seen from the diagram that the lower the fractional order coefficient, the higher the amplitude of the system vibration, the larger the resonance peak and the more uniform the increase.

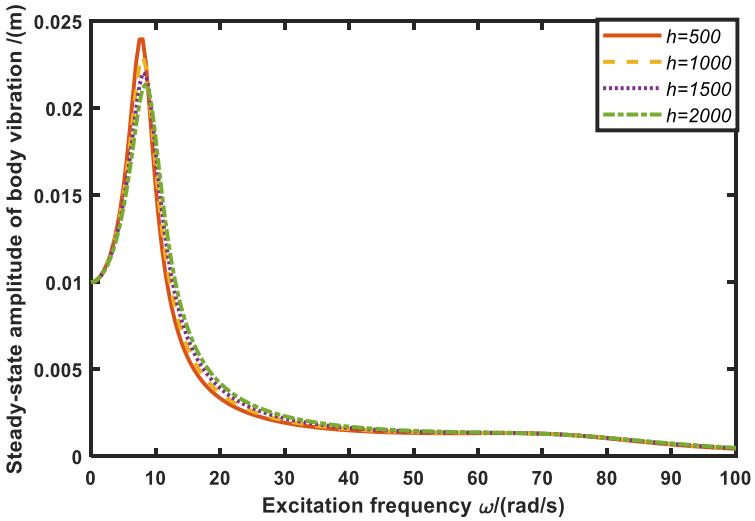

a) Amplitude-frequency response curve of body displacement

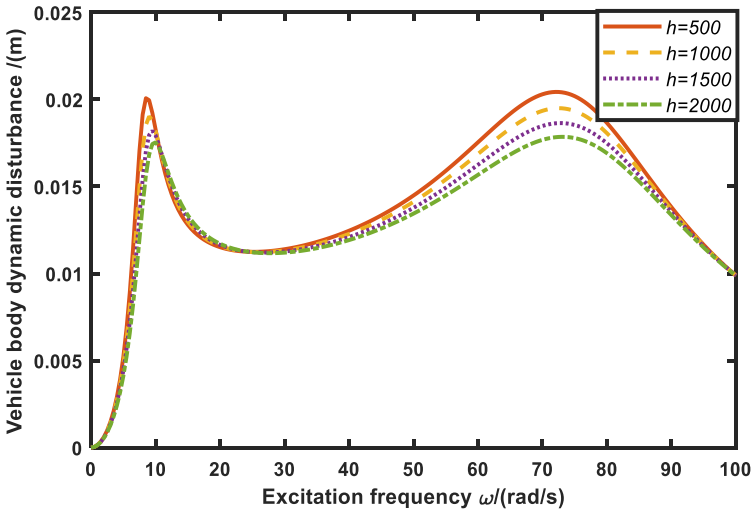

b) Amplitude-frequency response of suspension dynamic deflection

Fig.(8)Comparison of amplitude-frequency responses for different fractional order coefficients

4.3 Analysis of the influence of parameters on nonlinear characteristics

(1) Effect of Nonlinear Stiffness on Suspension Nonlinear Dynamic Performance

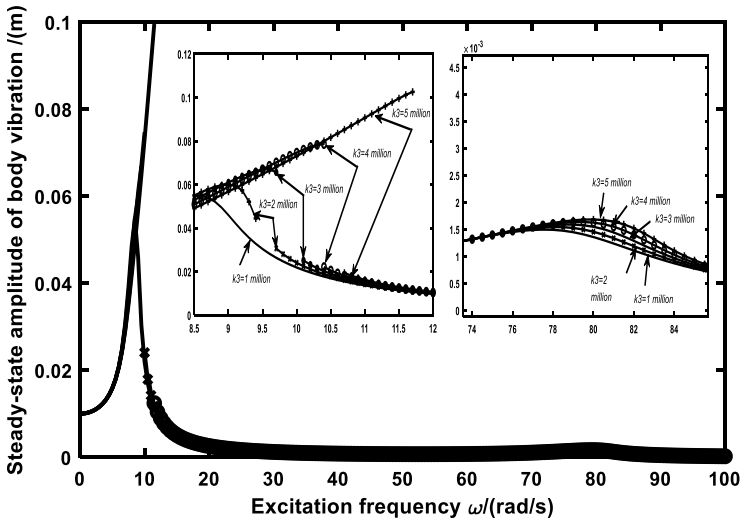

a) Amplitude-frequency response curve of body displacement

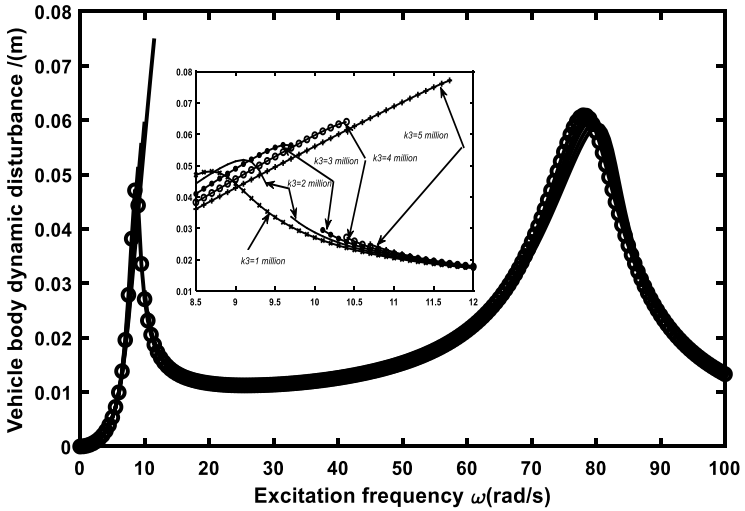

b) Amplitude-frequency response of suspension dynamic deflection

Fig.(9)Comparison of amplitude-frequency responses for different nonlinear stiffness coefficients

Because of the cubic stiffness term in the suspension, the system exhibits non-linear characteristics. IHBM is not only suitable for weak non-linear systems, but also for calculations of strong non-linear systems. By changing the value of cubic stiffness factor k_3, when k_3=1000kN/m,2000kN/m,3000kN/m,4000kN/m, 5000kN/m, the amplitude-frequency response curve is calculated as shown in Figure (9). Figure (9) shows that when the excitation frequency is low, the resonance peak tends to deflect to the right with the increase of k_3. The non-linear characteristics are not obvious at 1000kN/m. IHBM can also obtain continuous amplitudes. Starting from 2000kN/m, the amplitude-frequency response curve shows typical non-linear characteristics at the low-frequency resonance peak, exhibits multi-solution and discontinuous jumping phenomena, and bends to the high frequency. It can be observed that the vehicle suspension system is strongly non-linear under low

frequency excitation, and the resonance peak area should be avoided in the design to reduce the strong non-linear effect.

(2) Effect of external excitation amplitude on dynamic behavior of vehicle system

With k_3=3000kN/m and other parameters unchanged, the calculated amplitude-frequency characteristic curve is shown in Figure (10) when the excitation amplitudes are changed to F=0.006m, F=0.008m and F=0.01m respectively. It can be seen from the calculation that the excitation amplitude not only affects the resonance peak value of the suspension system, but also the higher the excitation amplitude, the more obvious the non-linear multi-value characteristics of the system. As shown in the figure , when F=0.01m, the coordinate points of the discontinuous region in the forward and reverse scanning can be known to have a binary region and when F is reduced the binary region no longer obvious. However, the excitation amplitude in the high frequency section will affect the resonance peak of the system obviously. The higher the excitation amplitude, the higher the resonance peak value, but the non-linear characteristics of the system are not obvious.

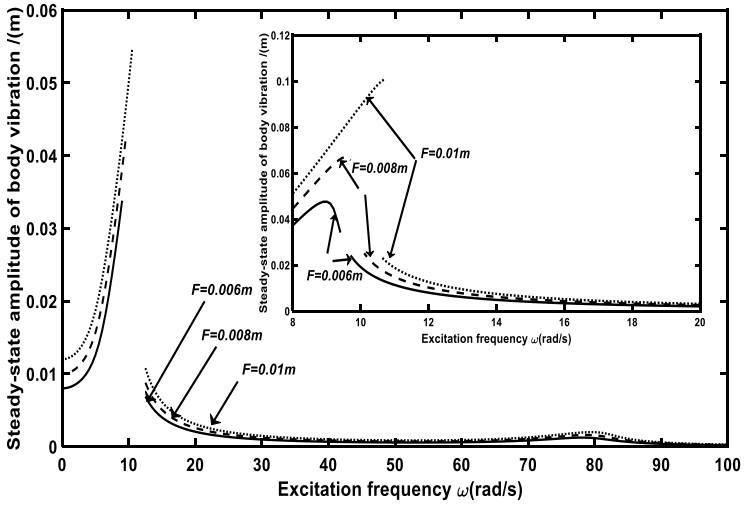

a) Amplitude-frequency response curve of body displacement

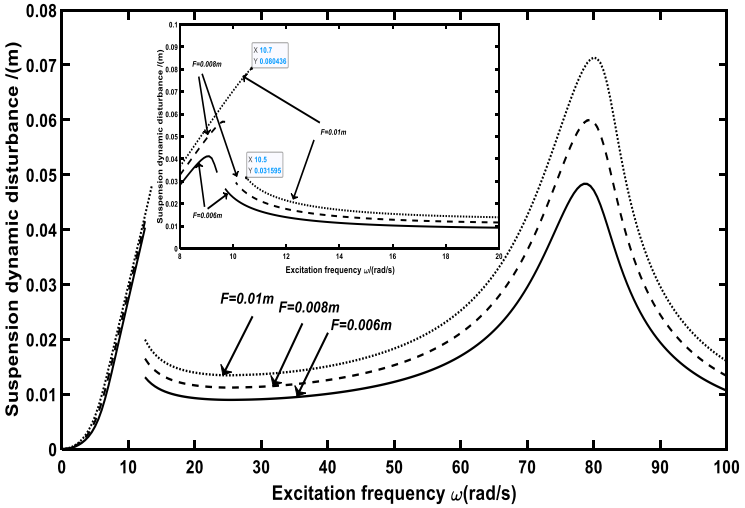

b) Amplitude-frequency response of suspension dynamic deflection

Fig.(10) Comparison of amplitude-frequency responses of different excitation amplitudes

(3) Effect of mass ratio on dynamic behavior of vehicle system

Under the constant condition of k_3=3000kN/m, when the body mass is changed to m_1=200kg, 220kg, 240kg, 260kg, 280kg, the calculated amplitude-frequency response curve is shown in Figure (11). It can be seen from the figure that the body mass change has almost no effect on the high-frequency resonance peak, but has a significant impact on the low-frequency resonance peak. As the mass increases, the resonance peak shifts to the left, and the nonlinear multi-value area tends to be more obvious. For example, when m_1=280kg and 240kg, the discontinuous position coordinates of forward sweep and reverse sweep appear in the figure. It can be noticed that the larger the body mass is, the larger the multi-value region appears.

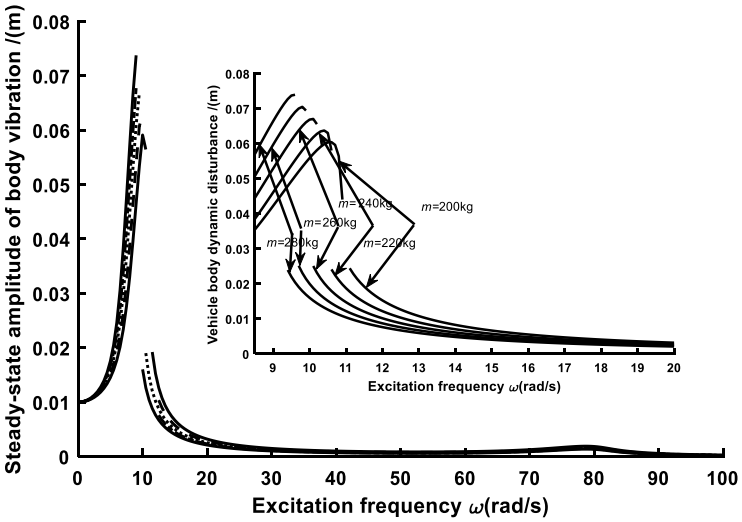

a) Amplitude-frequency response curve of body displacement

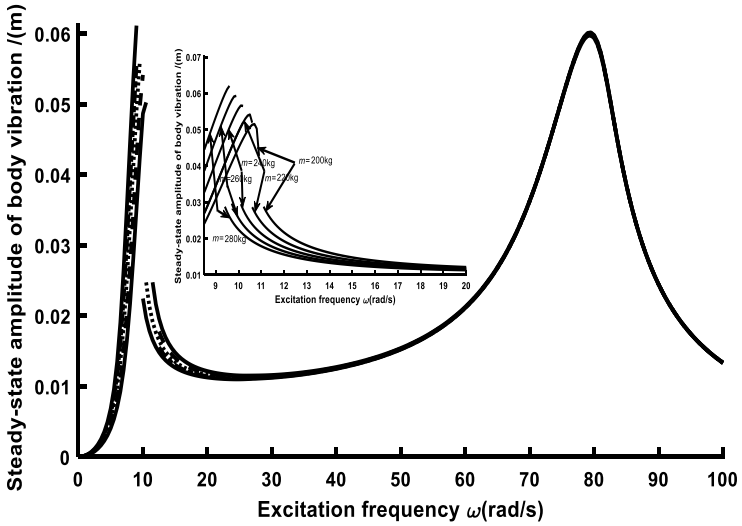

b) Amplitude-frequency response of suspension dynamic deflection

Fig.(11)Comparison of amplitude-frequency response of different body mass

(4) Effect of Tire Quality on Suspension Nonlinear Performance

When the tire quality is changed and m_2 = 30kg, 40kg, 50kg, 60kg, 70kg are taken, the amplitude-frequency response curve is calculated as shown in Figure (12). As can be noted from Figure (12), tire quality has no effect on low frequency resonance peak, and the amplitude-frequency characteristics of

the low frequency band are identical. Different quality tires in the low frequency band have a great influence on high frequency resonance peak. If the tire quality is different, the resonance peak frequencies are completely different and the non-linear characteristics of the system are not affected.

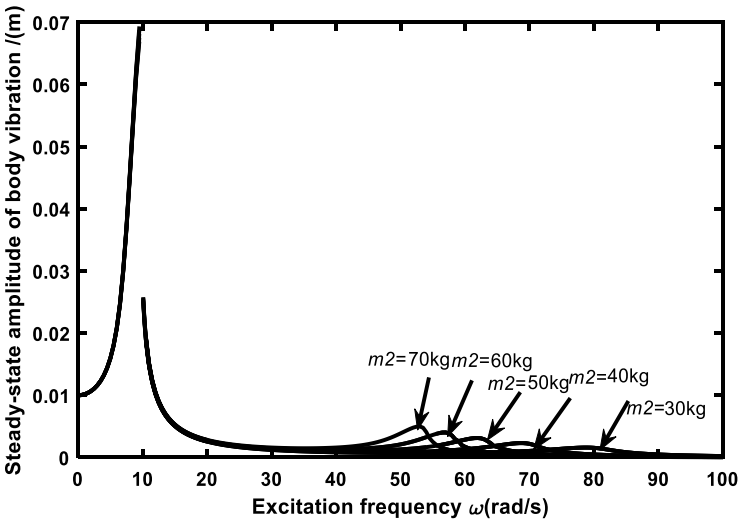

a) Amplitude-frequency response curve of body displacement

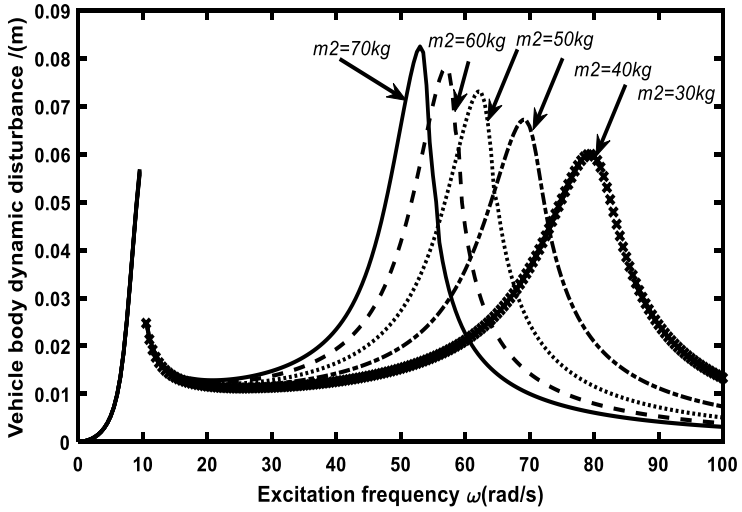

b) Amplitude-frequency response of suspension dynamic deflection

Fig.(13)Comparison of amplitude frequency response of different tire masses

5. Conclusion and analysis

This section presents the derivation of the general calculation format of the 2-DOF incremental harmonic balance method containing the fractional-order nonlinear system. The amplitude-frequency response characteristics of a two-degree-of-freedom nonlinear vehicle suspension system with fractional order under external harmonic excitation were studied by using this scheme. At the same time, the effects of fractional parameters and other variables on the nonlinear characteristics of the system are also studied, and the conclusions are as follows:

(1)The amplitude-frequency response characteristics of fractional-order differential order system are significantly affected by the order. The lower the fractional order, the higher the amplitude of system vibration and the larger the resonance peak value.

(2) The fractional-order differential coefficient has a significant impact on the system's amplitude-frequency response characteristics. The larger the differential term, the lower the resonance peak of the frequency response, which is quite different from the integer-order comparison.

(3) With the increase of the nonlinear term k3, the nonlinear characteristics of the system become more pronounced. The system obviously exhibits nonlinear characteristics, and unstable solution regions appear. Multi-value solutions are obtained when the frequency is swept in both directions. The resonance peaks tend to deviate to the right. The non-linear characteristic of low frequency band is more obvious than that of high frequency band.

(4) The influence of the excitation amplitude on the amplitude-frequency characteristics is studied. The larger the excitation amplitude, the greater the resonance peak value of the system, and the greater the excitation amplitude, the more significant the nonlinear characteristics in the low frequency band.

(5) The body mass has a significant influence on the low-frequency resonance peak and has no influence on the high-frequency resonance peak, while the tire quality has a significant influence on the high-frequency resonance peak and has no influence on the low-frequency resonance peak.

Funding

This study was funded by the National Natural Science Foundation of China (grant number 12072205).

Conflict of Interest

The authors declare that they have no conflict of interest.

Data Availability Statements

The datasets generated during and analysed during the current study are available from the corresponding author on reasonable request.

References

[1] Song, H.T. Study on time-delay vibration absorption control of fractional-order damped suspension system [D]. Zibo: Shandong University of Technology, 2016.

[2] Bagley, R. L. On the fractional calculus model of viscoelastic behavior[J]. Journal of Rheology, 1986, 30(1): 935-952.

[3] Moreau X , Oustaloup A , Nouillant M. The crone suspension[J]. Control Engineering Practice, 1996, 4(8): 1101-1108

[4] Sun, H.L., Jin, C., Zhang, W.M. Modeling and experimental analysis of oil and gas suspension based on fractional calculus[J]. Journal of Vibration and Shock, 2014, 33(17):167-172.

[5] Zhang, J.W., Chen, S.Z., Li, H.B., et al. Research on multi-branch hydro-pneumatic suspension model based on fractional order[J]. Chinese Journal of Automotive Engineering, 2015, 5(6): 408-414.

[6] Zhang, J.W., Chen, S.Z., Zhang, Y.Z., et al. Research on modeling of hydropneumatic suspension based on fractional order[J]. Mathematical Problems in Engineering, 2015, 2015: 1-11.

[7] Zhou, S., Song, G., Sun, M., et al. Nonlinear dynamic analysis of a quarter vehicle system with external periodic excitation[J]. Nonlinear Mech. 84, 82–93 (2016)

[8] Litak, G., Borowiec, M., Ali, M., et al. Pulsive feedback control of a quarter car model forced by a road profile[J]. Chaos Soliton Fract. 33(5), 1672–1676 (2006)

[9] Litak, G., Borowiec, M., Friswell, M.I., et al. Chaotic vibration of a quarter-car model excited by the road surface profile[J]. Commun. Nonlinear Sci. 13(7), 1373–1383 (2006)

[10] Türkay, S, Akçay, H. A study of random vibration characteristics of the quarter-car model[J]. Sound Vib. 282(1–2), 111–124(2005)

[11] Wang, S., Hua, L., Yang, C., Zhang, Y.O., Tan, X.D. Nonlinear vibrations of a piecewise-linear quarter-car truck model by incremental harmonic balance method[J] Nonlinear Dynamics.92(5), 1719–1732 (2018)

[12] Sheng, Y., Wu, G.Q. Quantitative study of automotive nonlinear suspension system based on incremental harmonic balance method[J]. TongJi University. (Natural. Science.) 39(3), 405–410(2011)

[13] Zhou, S., Song, G., Li, Y., Huang, Z., Ren, Z. Dynamic and steady analysis of a 2-DOF vehicle system by modified incremental harmonic balance method(Article)[J]. Nonlinear dynamics. 2019, Vol. 98(No.1):75-94.

[14] Zhou, S.H., Song, G.Q., Sun, M.N., Ren, Z.H., Wen, B.C. Dynamic interaction of monowheel inclined vehicle-vibration platform coupled system with quadratic and cubic nonlinearities[J] Mech. Syst. Signal Process. 412,74–94 (2018).

[15] Zhou, S.H., Song, G.Q., Sun, M.N., Ren, Z.H. Nonlinear dynamic analysis of a quarter vehicle system with external periodic excitation[J]. Non-linear Mech. 84, 82–93 (2016)

[16] Shen, Y.J., Wen, S.F., Li, X.H., Yang, S.P., Xing, H.J. Dynamical analysis of fractional-order nonlinear oscillator by incremental harmonic balance method[J]. Nonlinear Dynamics, 2016, 85(3):1457-1467.

[17] Shen, Y.J., Yang, S.P, Xing, H.J., Gao, G.S. Primary resonance of Duffing oscillator with fractional-order derivative[J]. Communications in Nonlinear Science and Numerical Simulation, 2012, 17(7): 3092-3100.

[18] Shen, Y.J., Wei, P., Yang, S.P. Primary resonance of fractional-order van der Pol oscillator[J]. Nonlinear Dynamics, 2014, 77(4):1629-1642.

[19] Shen, Y.J., Yang, S.P, Xing, H.J., et al. Primary resonance of Duffing oscillator with two kinds of fractional-order derivatives[J]. International Journal of Non-Linear Mechanics, 2012, 47(9):975-983.

[20] Chang, Y.J., Tian, W.W., Chen, E.L., et al. Hysteresis nonlinear dynamic model of metal rubber based on fractional differential [J]. Journal of Vibration and Shock, 2020,139 (04):233-241.

Moreau X., Onstaloup A. and Nouillant M. (1996). Comparison of LQ and CRONE methods for the design of suspension systems. Proceedings of IFAC'96 World Congress, San Francisco,California, USA June 30 - July 5.